Invisible Bactericidal Coatings on Generic Surfaces through A Convenient Hand Spray

Joey Andrew A. Valinton[a#], Alfin Kurniawan[a#], Ren-Huai Jhang[a], Christian R. Pangilinan[b], Che-Hsin Lee[b], Chun-Hu Chen[a]*

[a] Department of Chemistry, National Sun Yat-sen University, Kaohsiung, Taiwan 80424

[b] Department of Biological Science, National Sun Yat-sen University, Kaohsiung, Taiwan 80424

*E-mail: chunhu.chen@mail.nsysu.edu.tw

[#]contributed equally

Abstract

Robust antimicrobial coatings featuring high transparency, strong bactericidal activity, and easy application procedure on generic surfaces can be widely accepted by the public to prevent pandemics. In this work, we demonstrated the hand sprayer-based approach to deposit complex oxide coatings composed of Co-Mn-Cu-Zn-Ag on screen protectors of smartphones through acidic redox-assisted deposition (ARD). The as-obtained coatings possess high transparency (99.74% transmittance at 550 nm) and long-lasting durability against swiping (for 135 days of average use) or wet cleaning (for 33 days of thrice-a-day routine). The spray coating enabling 3.14% *E. coli* viability can further be reduced to 0.21% through a consistent elemental composition achieved via the immersion method. The high intake of Cu^{2+} in the coating is majorly responsible for bactericidal activity, and the presence of Ag^{+} and Zn^{2+} is necessary to achieve almost complete eradication. The success of extending the bactericidal coatings on other typical hand-touched surfaces (e.g. stainless steel railings, rubber handrails, and plastic switches) in public areas has been demonstrated.

Keywords: antibacterial coatings, oxide-based, spray deposition, bactericidal activities, transparent surfaces

Introduction

Stopping global pandemics is an important and urgent task for the scientific community.[1] Significant loss of life and economic activities causes severe impacts on countless families and individuals at every corner. Like all the pandemics recorded in history, close physical contact and poor disinfection on hand-touched surfaces always lead to the rapid transmission of germs and viruses, and ultimately to the uncontrollable pandemics.[2, 3]

Since smart devices (e.g. cell phones, watches, etc.) have been widely adopted in modern society and individuals, the touch-control panels, usually integrated with the monitor display, become a major hazard of disease transmission due to frequent touching in daily life. This makes the touch panel of smart devices to be a "transmission hub" to spread bacteria and viruses on all the other surfaces touched by human hands.[4] Therefore, antibacterial coatings on these panels could significantly inhibit disease transmission.[5, 6] Nevertheless, such the strategy may only work if the major population is willing to adopt antibacterial coatings on the surface of all kinds of smart devices. This posts the new criteria for the public willing to accept antimicrobial coating: high transparency, easy operation, generic depositing substrates, and long duration. Low transparency coatings shield or degrade the visual quality of the control display panels, almost impossible to convince the public to accept. Complicated coating procedures only compatible with specific substrates would face the same difficult situations. High durability of coatings, meanwhile, reduces the frequency to repair or reinforce the antimicrobial activities.

Inorganic antimicrobial coatings usually possess a longer duration to most chemicals and mechanical abrasion (e.g., scrubbing and regular cleaning) than their organic counterparts. Yet many of the well-recognized inorganic antimicrobial coatings are either too thick to be transparent or too intense in color (e.g. Cu, Ag, or stainless steel surfaces).[7] In this regard, metal oxide-based ultra-thin coatings are a reasonable choice to afford high stability and transparency toward antimicrobial coatings.

Well-reputed deposition methods like chemical vapor deposition (CVD), physical vapor deposition (PVD), and atomic layer deposition (ALD) are simply too complicated for the public.[8-11] Although solution-based deposition techniques generally feature with

easy operation, typical examples of sol-gel, dip-, spin-coating, and drop-casting still need high temperature annealing to consolidate the adhesion of coatings on substrates.[12-15] The public interests may be significantly decreased due to the inconvenience of additional heating step, and also forbidden toward some soft-substrate devices with low thermal durability. Ambient deposition procedures capable of achieving strong adhesion on generic substrates are therefore highly preferred.[1]

Typically, copper, zinc, and silver cations have intrinsic antimicrobial activities against a wide spectrum of bacteria, viruses, and other microorganisms,[16, 17] which can be caused by disruption of cell membranes/coatings,[18-20] or oxidative damage due to reactive oxygen species.[21-23] Thus, a thin metal oxide layer containing these three bioactive metals is proposed to provide exceptional antimicrobial activities. In the literature, these cations have been successfully incorporated into oxide-based coatings for bone implant [24, 25] and stainless steel substrates.[4] Nevertheless, easy procedures capable of combining all these cations into one continuous, invisible coating have been too challenging already.[10, 26, 27] This would be even more difficult with the criteria of room-temperature conditions on generic substrates.

To address all the criteria above, the earlier works of acidic redox-assisted deposition (ARD) have been shown to be capable of producing uniform, continuous, and void-free metal oxide thin films with strong adhesion.[28] Such technique can be applied on diverse substrates such as wood, glass, or metal among others, through simple immersion onto the deposition mixture in the ambient conditions.[7, 28-30] Compared to the well-known alkaline precipitation where oxidation states of metal cations remain the same, ARD and the precipitation approaches (ARP) are emerging alternatives uniquely featured with tunable oxidation states, homogeneous multi-element distribution, and strong adhesion without the needs of thermal annealing. In addition, the ARD oxide coatings can incorporate from two (Co-Mn, Cu-Mn),[7, 28, 29] three (Fe-Co-Mn),[28] and up to four (Ag-Ce-Fe-Mn) [30] different metal cations in a single layer. Following the simplicity and versatility of the technique, we propose that ambient-condition ARD is promising to dope all the antimicrobial active cations in one coating via an intuitive, convenient method for the public, such as hand sprayer.

In the present study, we have successfully realized transparent bactericidal coatings via hand spray-based approach under ambient conditions for 15 min. The as-generated five-metal oxide coatings exhibit transmittance values of 99.74% with a strong adhesion on screen protectors of smartphones. The high bactericidal activity against *E. coli* (with viability at 3.14%) has been observed. The films exhibit strong durability and retain bactericidal activities against the finger swiping and wet cleaning for at least a month. The incorporation of Cu^{2+} is responsible for the major activities, while the presence of Ag^{+}, Zn^{2+} are crucial to achieve nearly 100% bactericidal activity, as compared to only Cu^{2+} doping cases. We further demonstrated the success of realizing this bactericidal coating on other typical hand-touched surfaces (e.g. stainless steel railings, rubber hand rails, and plastic switches) commonly seen in public areas.

Experimental Section

Hand Spray-Based Approach

Two solutions were prepared for the hand spray-based approach. Solution A is mainly prepared by adding 0.04 mmol cobalt (II) acetate tetrahydrate [$Co(CH_3COO)_2 \cdot 4H_2O$; 98%; Alfa Aesar] in 100 mL deionized water. The addition of bactericidal metals was done by spiking Solution A first by 0.08 mmol copper (II) nitrate trihydrate ($Cu(NO_3)_2 \cdot 3H_2O$; 99%; Sigma-Aldrich), then by 0.08 mmol zinc (II) nitrate hexahydrate ($Zn(NO_3)_2 \cdot 6H_2O$; 98%; ACROS), and lastly by 0.08 mmol silver nitrate ($AgNO_3$; ≥99.8%; AENCORE). Solution B was prepared by dissolving 0.013 mmol potassium permanganate ($KMnO_4$; ≥99%; J.T. Baker) in 100 mL deionized water. These were contained in PET spray bottles ready for the spray coating. The tempered glass screen protector substrates were removed of its plastic cover before use, while the stainless steel (5 cm × 5 cm), rubber handrail (~5 cm × ~5 cm) and electric switch sample substrates were not subjected to specific cleaning steps. Microscope glass slide substrates were subjected to washing (with soapy water, deionized water, acetone, and isopropanol) and blow-drying prior to use. Indium tin oxide (ITO) substrates were washed (with concentrated nitric acid, water, acetone, and isopropanol), dried, and plasma-treated prior to deposition. For the spray process, Solution A was first sprayed directly onto the substrates at a 90º angle for at most five spray shots, or until the solution predominantly coats the entire surface. This was followed by spraying of Solution B in the same manner. The substrates were left undisturbed for 15 minutes. To simulate the potential, direct application on electronics, a damp Kimwipe was used to remove the liquid on the substrates, followed by wiping it dry with another sheet. For multiple coats, the same process above was repeated.

The Immersion-Coating Approach

For the immersion method, both Solutions A and B (50 mL for each) are mixed in a 250-mL beaker. Afterwards, the substrate (ITO glass) that was taped (using a double-sided tape) under a floating object (expanded polystyrene block), and with the coating side

face-down for a direct contact with the precursor solution for a film-growth time of 15 minutes. The immersion-coated ITO was then rinsed with water and dried under N_2 stream prior to use. We named this series of immersion-method oxide coatings with "-IOC" suffix to be distinguished from the spray coating samples. To create the two-metal oxide coating (CoMn-IOC), only Co^{2+} and MnO_4^- precursors were used into the growth solution. The growth solutions for the cases of three-metal (CoMnCu-IOC) and the four-metal (CoMnCuZn-IOC) coatings were prepared by additionally spiking the corresponding cation precursors (0.80 mM each) into the growth solutions of CoMn-IOC. The coating containing all the five metals is named as CoMnCuZnAg-IOC.

Coating Characterization

The transparencies of the coated glass substrates were measured using a JASCO V-630 Double-beam UV-Vis Spectrophotometer. For the surface analysis, X-ray Photoelectron Spectroscopy (XPS) measurements were done using a VG ESCALAB 250 Spectrometer measured using an Al Kα source. The microstructural images were taken using an FEI Inspect F50 Scanning Electron Microscope.

Durability Tests

The durability test setup was made by putting a rubber eraser (or a water-wet Kimwipe) under a 100 g weight and was placed over a spray-coated microscope glass slide (see Figure 2a). A swipe was done by pulling the glass slide out of the weighted setup. The setup was then repositioned over the glass slide again to repeat for 100 times. The retained concentrations of Cu, Ag, and Zn were solved following this equation:

$$\%\ \text{concentration} = \frac{I_f - I_i}{I_i} \times 100\% \quad (1)$$

where I_f and I_i are the initial (zero swipes) and final (after 100 swipes) relative intensities of the Cu $2p_{3/2}$, Ag $3d_{3/2}$, and Zn $2p_{3/2}$ peaks in their high resolution X-ray photoelectron spectra.

Bactericidal Tests

The bactericidal activities of each glass sample were evaluated based on the colony counting method using Gram-negative *Escherichia coli* DH5-α as the model bacteria. All the experimental procedures were performed following a standard [ISO 14729:2001]. The bacterial suspension was grown in Luria–Bertani (LB) medium (Sigma-Aldrich, pH 7.4) and incubated at 37 °C with gentle shaking for 16 h to reach stationary phase. Subsequently, aliquots of the bacteria culture were drop-casted onto the sample surfaces at a density of 10^4 CFU per mL, followed by incubation at 37 °C for 6 h (12 h for the immersion-coated ITO samples). After incubation, the substrates with the bacterial inoculum were immersed in fresh LB medium and sonicated for 3 min to detach the bacteria adhering to the surface. Aliquots (100 μL) of the diluted bacteria suspension in phosphate buffered saline were then plated on LB agar and incubated at 37 °C overnight. All the bactericidal tests were performed in triplicate for each sample and the results are expressed as mean ± standard deviation (SD). The bacterial viability was determined by counting the colony numbers on LB agar plates from appropriate bacterial dilution and percent viability was obtained according to the following equation:

$$\%\ \text{viability} = \frac{N_s}{N_{ctrl}} \times 100\% \qquad (2)$$

where N_{ctrl} and N_{s} represent the average number of bacterial colonies in the uncoated (control) and coated substrates, respectively.

Results and Discussion

The chemical principle of the ARD coating is based on the redox reaction between cobalt (II) acetate (the reductant) and potassium permanganate (the oxidant) in water (Eq. 3), where the strong oxidative ability of $KMnO_4$ acting on a top surface of generic substrates provides a robust coating adhesion.[28, 31]

$$9\ Co^{II}{}_{(aq)} + 3\ Mn^{VII}O_4^-{}_{(aq)} + 14\ H_2O_{(l)} \rightarrow Co^{III}{}_9Mn^{IV}{}_3O_{26}H_{13\,(s)} + 15\ H^+{}_{(aq)} \quad (3)$$

The products of cobalt manganese oxyhydroxide ($Co^{III}{}_9Mn^{IV}{}_3O_{26}H_{13}$, denoted as CMOH) have been shown to be a highly continuous film with a thickness as small as tens of nanometers, enabling high transparency with full surface coverage.[29] The acidic nature of the reaction mixture avoids the occurrence of alkaline precipitation.[32] The oxidant MnO_4^- is most likely to perform a rapid corrosion on the substrates to gain strong adhesion.[28] Meanwhile, the oxyhydroxide layer formation behavior has been observed to be dependent on the counter-anions of the metal precursors, where the mechanism studies show a self-limiting role of acetate anions during the film growth.[28] Hence, the usage of acetate as the counter-anion of the Co precursor should enable regulation on the film thickness for the high transparency purpose.

Incorporation of other foreign cations during the formation of CMOH coating is known.[28, 30] Whereas a redox reaction (Eq. 3) is fundamental for the deposition, earlier reports have not only exhibited successful inclusion of oxidizable metal ions like Co^{2+}, Fe^{2+}, and Ce^{3+} through inner-sphere intermediates with the anionic oxidant [26] (in this case, MnO_4^-), but also individual inclusion of oxidation-inert metals like Cu^{2+} or Ag^+ in significant amounts. So we doped antimicrobial-active cations into CMOH to yield antibacterial coatings.

The Hand Spray Based Approach

In a typical deposition procedure, two spray solutions are needed. The first solution, denoted as Solution A, is an aqueous mixture containing Co^{2+}, Cu^{2+}, Zn^{2+}, and Ag^+; while

the other one, denoted as Solution B, is a $KMnO_4$ aqueous solution. The separation of Co^{2+} and $KMnO_4$ in two different hand sprayers is the key to trigger the deposition only when the two solutions are mixed. The ratio of Co^{2+} to MnO_4^- was kept at 3:1 as the ideal stoichiometric ratio as shown in Eq. 3, while the other metal cations are twice the Co concentrations. We chose tempered glass screen protectors as the main substrates due to the wide use by the public for diverse smartphones.

The hand sprayer-based procedure starts with spraying Solution A to cover the entire surface of screen protectors, followed by another spraying of Solution B in the same manner. After a 15-min aging under ambient conditions without any heating step, the mixed solutions can be cleaned by water rinse washing or paper wiping until completely dry. Then, a highly transparent and almost invisible coating has been deposited on the substrates, as demonstrated in Figure 1.

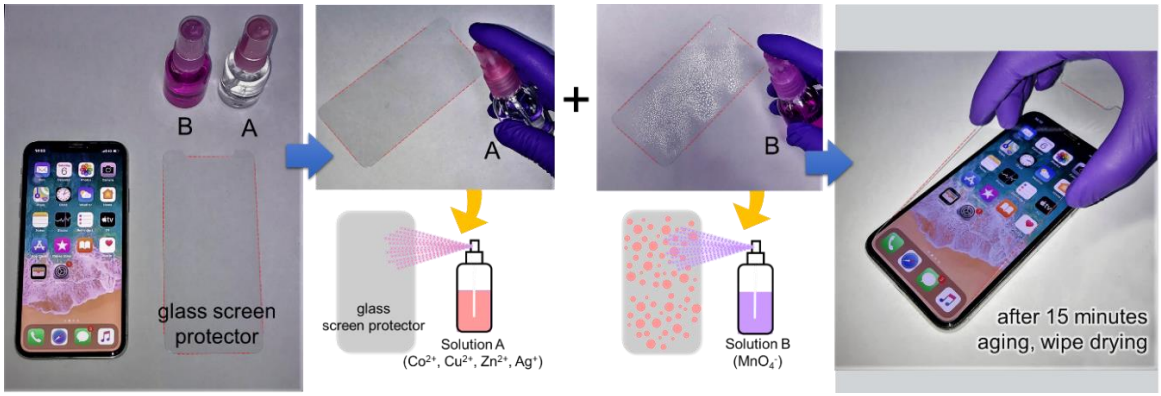

Figure 1. The hand-sprayer coating demonstration on a smartphone screen protector. Solution A (containing Co^{2+}, Cu^{2+}, Ag^+, and Zn^{2+}, colorless) and Solution B (containing MnO_4^-, pink) were sprayed consecutively on top of the glass screen protector. After aging at room temperatures for 15 min, the solution mixture on the protector was removed to obtain the CoMnCuZnAg oxide coatings.

The transparency of the hand sprayer-coated screen protectors is almost identical to the uncoated ones (Figure 2a). The optical transmission spectra collected (Figure 2b) from the five different locations show nearly the same transmittance values, suggesting a highly uniform coverage over the entire top surface. The statistical values of transmittance

at 550 nm are 99.74 ± 0.17%, just slightly lower than the uncoated ones. Moreover, all the metals incorporated are present on the coated surface, as analyzed via X-ray photoelectron spectroscopy (XPS, see Supporting Information, Figure S1).

To test the bactericidal performance of the hand sprayer-coated glass as a proof of concept, we performed a bacterial viability test using *E. coli*, a common pathogen seen on smartphones, through incubating a bacterial solution on the surface for time (12 and 24 h, respectively) before transferring to agar plates for colony counting. The hand sprayer-coated glass shows a significant decrease of viability (3.14 ± 4.22%) compared to the uncoated one (100 ± 12.33%), realizing the immense bactericidal activity (Figure 2c). Such the activity is comparable to other bactericidal coatings in literature, as well as those commercially available (Table S1). On one hand, the uncoated culture plates (insets of Figure 2c) show live bacteria colonies (white spots) after 12 h (i), which multiplied after 24 h (ii), indicating further bacterial proliferation; on the other hand, almost no sign of bacterial growth is seen in the hand sprayer-coated glass cultures after 12 h (iii) and becomes virtually clean after 24 h (iv). Overall, this proves the bactericidal efficacy of the hand sprayer-coated surface.

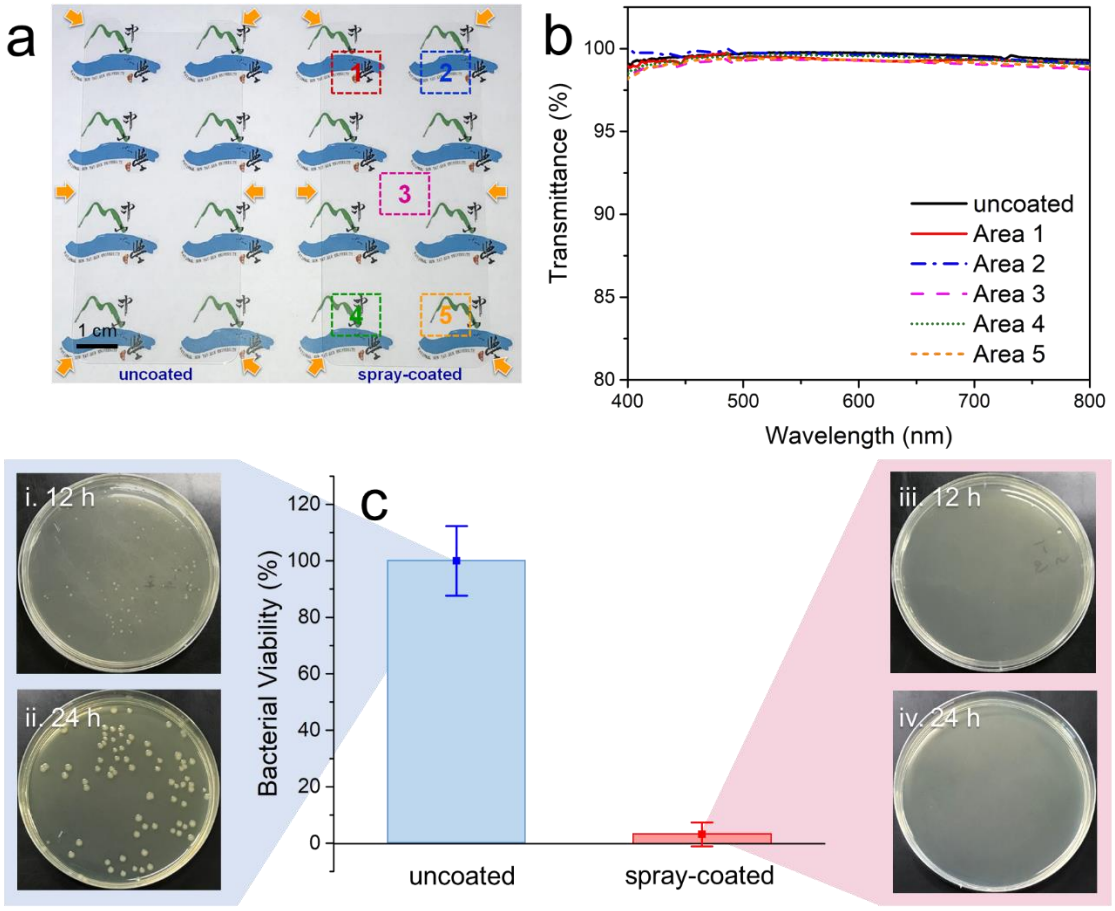

Figure 2. Properties of the hand sprayer coatings on a smartphone screen protector. (a) The appearance comparison of the uncoated and the spray-coated screen protectors. (b) The visible light transmittance profiles of the locations corresponding to the area denoted as 1-5 indicated in (a). (c) The bactericidal activity (in percent viability of *E. coli*) of the spray-coated versus the uncoated screen protectors; bacterial cultures show colony growth on uncoated [(i) and (ii)] and spray-coated [(iii) and (iv)] ones at different times (12 h and 24 h, respectively).

To test the coating durability against swiping, a setup composed of a rubber eraser pressed down by a 100 g weight (corresponding to a pressure of 2.31 kPa) was used (Figure 3a). Pressurized swiping was simulated by pulling the hand sprayer-coated glass while holding the setup in place. After 100 swipes, the samples show the retained loadings of Ag

and Zn decreased to 60.44, and 44.42%, respectively, while the Cu one is highly preserved to be 99.04% (Figure 3b). Relating to the average finger swiping pressure of 0.5 kPa [33] the projected complete removal of Ag, Zn, and Cu should occur after 940, 1,321, and 48,300 swipes, respectively. Hence, the bactericidal coating may remain for ~185 days based on the daily average swiping interactions by the public on mobile devices (2,617 swipes a day). [34] In terms of dermal contact, the maximum amount of the metals deposited in a single coat accounts only to 0.014% (for Cu and Zn), and 0.289% (for Ag) of their respective lethal doses (in mg metal/kg body weight) which ensures safety of usage (See Supporting Information, Table S2). The durable retention of the film is consistent with those of ARD-coated substrates that can resist 100 times peeling-off using adhesive tape,[28] as well as coated stainless still resisting multiple abrasions by a rubber ball.[7] This suggests the excellent adhesion of the ARD-based coating on the substrate regardless of the transparency level and/or thickness.

Meanwhile, the retention of the coating during frequent cleaning/disinfection routines is also essential to inspect.[1] To exhibit this, we replaced the rubber eraser in the setup (Figure 3a) with a water-damped Kimwipe, where the Ag, Cu, and Zn contents decreased by 45.5%, 33.9%, and 51.7%, respectively, after 100 swipes at 2.31 kPa (Figure 3b). According to the World Health Organization (WHO), high touch surfaces must be disinfected at least three times daily; [35] hence, 100 wipes would be equivalent to ~33 days of routine cleaning. This means that the antibacterial activities of the hand sprayer-based coatings may survive under the suggested disinfection routines for a month. Previously, Cu^{2+}/MnO_4^--based ARD coating on stainless steel exhibits as high as ~44% leaching of Cu^{2+} upon continuous water exposure for 500 minutes.[7] These leached ions are argued to result in bacterial cell death through ingestion,[1, 6, 7] outweighing the slightly compromised durability of the coating. Nevertheless, regulating the release of the metal ions (i.e. introducing other anions that can manipulate dissolution) may prospectively improve the lifetime of the coating. As such, the observed dissolution of metal ions is quite advantageous towards the bactericidal action.

The effect of reinforcing the hand sprayer-based coating through multiple layering was also studied to observe whether the transparency becomes compromised. Derived from the transmittance graphs (Figure 3c), by repeated layering up to seven-times, the

transmittance values at 550 nm (the inset in Figure 3c) are still as high as 99.33%. On average, every layer of deposition only decreases by 0.07% of transmittance. Accordingly, zero transmittance would require a more than 1000-times coating, suggesting that the degraded color and image quality in the spray-coated display panels are unlikely to occur. Thus the hand sprayer-based approach could be relatively easy to be accepted by the general public.

The chemical stability of both the spray solutions were inspected by UV-vis spectroscopy. Although Solution A remains highly stable in the tests, $KMnO_4$ in Solution B could undergo gradual self-decomposition upon exposure to light and heat. The loss of the purple color and the presence of dark precipitates indicate a deactivation and may result in an invalid spray solution.[36] Under the dark, cool environments, the loss of MnO_4^- is 0.77% per day (Figure 3d), while 11.07% loss of that per day was observed under sunlight. The use of the amber bottle to increase the chemical stability of photosensitive $KMnO_4$, shown by a loss of 0.98% per day (Figure 3d). The projected shelf life of solution B until full oxidant depletion would be 9 days under sunlight, or 129 days if stored indoors. Nevertheless, the public users must pay attention to the shelf-life of solution B to ensure the quality of the hand-sprayer coating.

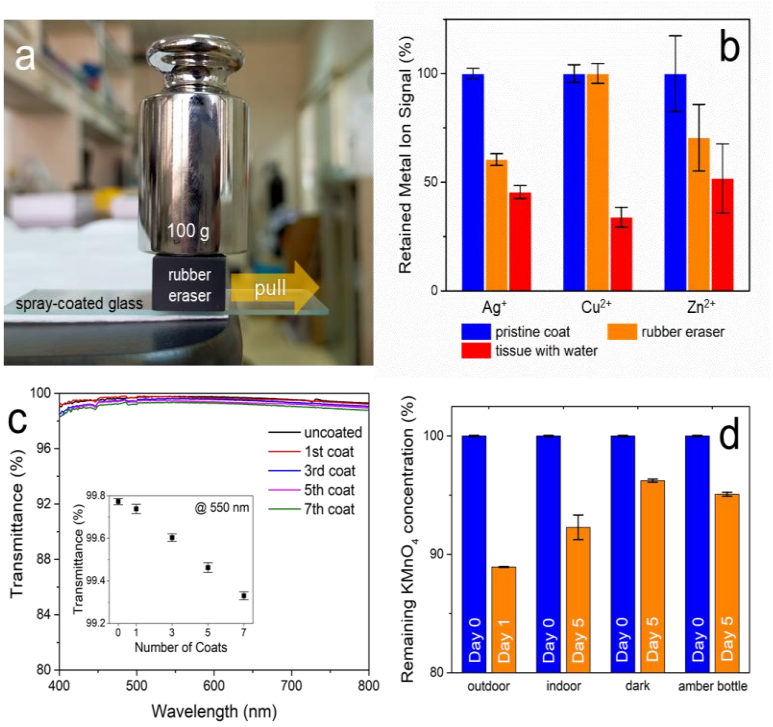

Figure 3. Properties of the hand-sprayer based coated glass. (a) The procedure for rubbing the coated glass with a rubber eraser with a pressure of 100 g, equivalent to 2.613 kPa and ~5 times the pressure of finger tapping on a smartphone). (b) The XPS results for the percentage of the Ag^{+}, Cu^{2+}, and Zn^{2+} in the coating after rubbing with a rubber eraser and a wet tissue using the setup in (a). (c) The UV transmittance of the glass upon multiple applications of the hand-sprayer coating; inset shows the transmittance values (at 550 nm) being lowered by the increased number of coats. (d) The percentages of $KMnO_4$ remaining in Solution B after exposure to different conditions, based on the absorbance at 525.5 nm wavelength (the λ_{max} of $KMnO_4$).

We further attempt to extend the generality of the antibacterial coatings on various high-risk surfaces in public places and healthcare facilities, including rubber handrails of escalators (Figure 4a), stainless steel objects (e.g. kitchenware, doorknobs, etc., Figure 4b), and finger-touch switches (e.g. light switch, elevator control panels, Figure 4c). These three examples were chosen to represent three typical categories of materials (i.e. rubbers, metals, and plastics), widely used for all kinds of hand-touch surfaces in our modern civilization.

The successful deposition of the coating is corroborated by the presence of the multiple cations in the XPS data (Figure S2), revealing the presence of all constituent metals on the tested surfaces. In agreement with the previous test results of the coated glass screen protector, no observable change in visual appearance was seen from these surfaces before and after the hand sprayer-based coating. These high transparent features may encourage the public's willingness to apply the ARD antibacterial coatings on surfaces, compared to masking object surfaces by a non-transparent layer (such as Cu foil, antimicrobial paint, and others)[37-39] for antibacterial purposes.

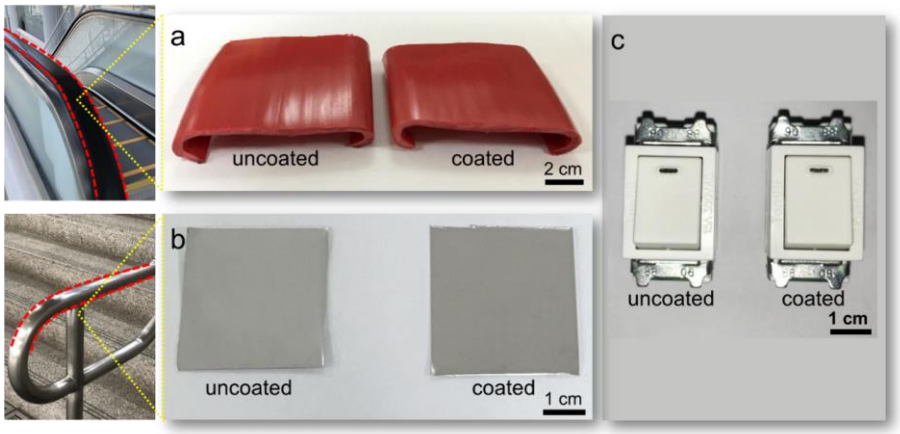

Figure 4. Applicability of the hand-sprayer based coating on various surfaces. The appearances of the surface before and after spray coating on (a) rubber surface as escalator handrails, (b) stainless steel surface as stair rails, and (c) electric switch surface.

The Metals on the Coating and Their Contributions to Bactericidal Activity

In order to understand the contribution of each metal cation to the bactericidal efficacy, we conducted a spike addition-like approach to produce a series of designed compositions as two-metal (Co and Mn), three-metal (Co/Mn/Cu), four-metal (Co/Mn/Cu/Zn), and five-metal (Co/Mn/Cu/Zn/Ag) cases. Yet the hand sprayer-based approach is not reliable enough, since a significant loading uncertainty may be caused from user to user. Alternatively, we adopted an "immersion" route as a much more reliable and

repeatable version of preparation to generate samples with well-controlled compositions. In brief, the substrates were floated on the top of the precursor solution mixture (same recipe as mixing Solution A and B) for the same preparation time at room temperatures. This method was designed to mimic the limited mass transport of the precursor mixtures on the substrates in the hand sprayer-based method. These immersion-route-made oxide coatings (i.e. the IOC series) following the spike-addition manner are denoted as CoMn-IOC (two metal case), CoMnCu-IOC (three metal case), CoMnCuZn-IOC (four metal case), and CoMnCuZnAg-IOC (five metal case).

The transparency of CoMnCuZnAg-IOC is similar to both the spray-coated ones and the pristine substrates, as recognized by the naked eyes (Figure 5a-c). Such the observation remains the same in the microstructural morphology revealed by the scanning electron microscope images (Figure 5d-f). The transmittance values of the hand sprayer- and immersion-coated samples at 550 nm (using the pristine glass sample as blank) are 99.62 ± 0.39% and 98.91 ± 0.20%, respectively (Figure 5g). The XPS data (Figure S3) of CoMnCuZnAg-IOC show the composition variations (i.e. elemental ratios among each element) less than 2.62%, much more reproducible than those produced by the spray method.

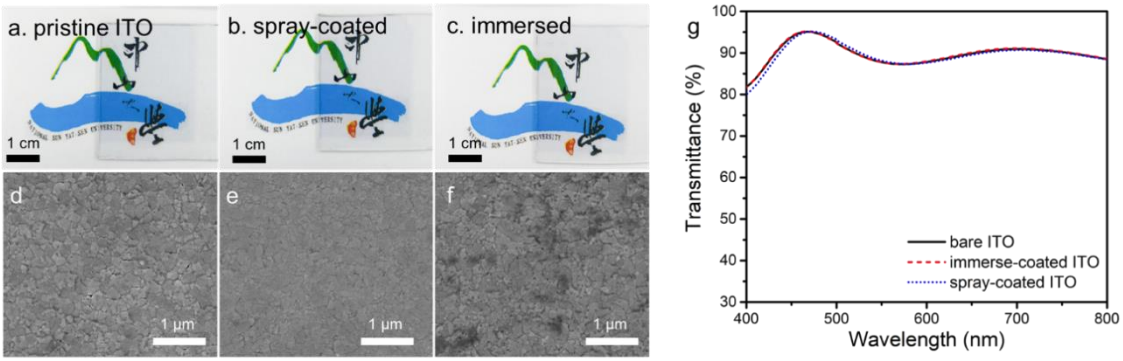

Figure 5. The comparison of the samples prepared by the hand sprayer-based approach versus the immersion-based approach (i.e. CoMnCuZnAg-IOC) on ITO. The comparison of the physical appearance of the (a) pristine, (b) hand sprayer-coated, and (c) CoMnCuZnAg-IOC -coated ITO, and their corresponding SEM images [(d), (e), and (f), respectively]. (g) The transparency results of the three ITO samples.

By directly conducting *E. coli* viability tests on these IOC samples, the antibacterial activities of each element can be more accurately evaluated. Figure 6a indicates an increase in the order of antibacterial activities of CoMn-IOC (60.14% viability), CoMnCu-IOC (27.34%), CoMnCuZn-IOC (12.59%), and CoMnCuZnAg-IOC (0.21%), which is consistently observed in the bacteria cultures (Figure 6b-f). In CoMn-IOC, the bactericidal effect is contributed by both Co [35] and Mn [40, 41] as a bacterial cell membrane disruptor. The spiking of Cu significantly lowers the bactericidal viability by 32.80%, greater than that by spiking of Zn (14.75%) and Ag (12.38%). If under the same concentrations, Ag and Zn should have intrinsically higher antibacterial activities than Cu.[42-45] But in this case, Cu^{2+} is observed to have higher quantities in the coating than the other two metals (Table S3), which means that the high bactericidal activity should come from the dominated quantity instead of the intrinsic properties. As such, the presence of Zn and Ag, even in much smaller contents, is necessary to achieve nearly 100% bactericidal activities, hence giving a higher advantage for a multimetal coating.

To provide direct cause of bacterial cell death on the bactericidal activity of CoMnCuZnAg-IOC, the morphological characteristics of remnant *E. coli* bacteria adhered on the coatings were examined by SEM (Figure 6g-h). The adhered *E. coli* cells on the uncoated ITO have intact rod-like morphology with a smooth cell membrane (marked with red dashed line) and flagellar filaments,[46] (marked by a yellow arrow), characterizing the normal growth of bacteria on this surface (Figure 6g). In stark contrast, the *E. coli* cells attached on the five-metal coating show the round or irregular shapes (orange arrows in Figure 6h), which are smaller (average of ~0.15 μm in diameters) compared to those in Figure 6g (average of ~3.5 μm), as well as defective cell membrane and wrinkled surface. Such differences suggest the rupturing of the bacterial cell membrane could be the main bactericidal action.[16-18, 47]

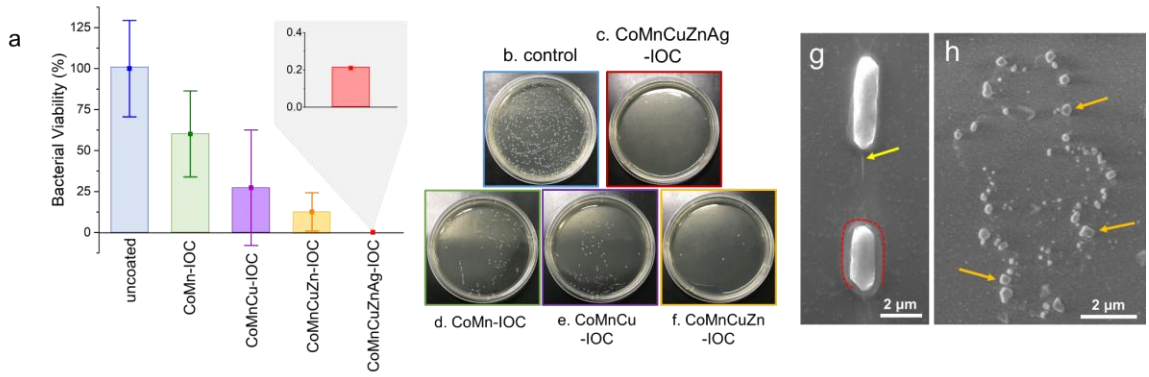

Figure 6. Inhibition of *E. coli* growth in the immersion-grown multimetal oxide films on indium tin oxide glass. (a) The percentage viability on various oxide coatings with different metal combinations; the inset shows the magnified percentage in CoMnCuZnAg-IOC. The culture plates containing the bacterial colonies remaining in the glass after 24 hours in the (b) uncoated, (c) CoMnCuZnAg-IOC, (d) CoMn-IOC, (e) CoMnCu-IOC, and (f) CoMnCuZn-IOC samples. The bacterial growth in (c), (d), and (e) comes from a more diluted culture of recovered live bacteria than those in (a) and (b). The SEM images of the remnants of bacteria on (g) uncoated ITO substrate, showing the intact flagellum (yellow arrow) and cell membrane (red dashed border), while that on the CoMnCuZnAg-IOC-coated glass (h) showing bacterial fragments (orange arrows).

Conclusions

In summary, we have demonstrated a versatile and convenient hand sprayer-based approach on yielding transparent surfaces that afford potent bactericidal activities. The durability, along with the re-applicability of the coatings without compromising transparency, provides the reliable, long-term protection. Compared to the usual options, the features of this coating strategy should integrate well into the common practices of the general public, and thus could significantly benefit public healthcare against severe pandemics. Following the proof of concept, we welcome further studies on upgrading this approach towards attaining versatile efficacy against other fomite-transmissible pathogens, including gram-positive bacteria and viruses (i.e., SARS-CoV-2) for a more practical prevention measure against current and future pandemics.

ASSOCIATED CONTENT

SUPPORTING INFORMATION

The Supporting Information is available free of charge at https://pubs.acs.org.

Bactericidal comparison table, X-ray photoelectron spectroscopy results of the coatings, Coating concentration comparison with lethal dose, Elemental composition data (PDF)

AUTHOR INFORMATION

These authors contributed equally: Joey Andrew A. Valinton and Alfin Kurniawan

CORRESPONDING AUTHOR:

Chun-Hu Chen – Department of Chemistry, National Sun Yat-sen University, Kaohsiung, 80424 Taiwan; E-mail: chunhu.chen@mail.nsysu.edu.tw

COMPETING INTERESTS

The authors declare no competing interests.

AUTHOR CONTRIBUTIONS

C.-H.C. initiated the concept and provided the funding of this work. J.A.V., A.K., and R.-H.J. made the samples and collected the data. J.A.V. and A.K. and C.-H.C. analyzed the data. C.R.P. and C.-H.L. conducted the biological tests and analysis. J.A.V. and A.K. and C.-H.C. wrote and edited the paper.

ACKNOWLEDGMENTS

We acknowledge the financial support from the Ministry of Science and Technology, Taiwan (Project MOST 109-2628-M-110-001-MY3). We would like to thank D. E. Gracilla and R. E. dela Peña, Jr. for their valuable inputs in the antibacterial tests.

References

1. Huang, H.; Fan, C.; Li, M.; Nie, H.-L.; Wang, F.-B.; Wang, H.; Wang, R.; Xia, J.; Zheng, X.; Zuo, X.; Huang, J., COVID-19: A Call for Physical Scientists and Engineers. *ACS Nano* **2020,** *14* (4), 3747-3754.
2. Infection prevention and control of epidemic-and pandemic prone acute respiratory infections in health care. https://apps.who.int/iris/bitstream/handle/10665/112656/9789241507134_eng.pdf.
3. Otter, J. A.; Donskey, C.; Yezli, S.; Douthwaite, S.; Goldenberg, S. D.; Weber, D. J., Transmission of SARS and MERS coronaviruses and influenza virus in healthcare settings: the possible role of dry surface contamination. *J. Hosp. Infect.* **2016,** *92* (3), 235-250.
4. Brady, R. R. W.; Verran, J.; Damani, N. N.; Gibb, A. P., Review of mobile communication devices as potential reservoirs of nosocomial pathogens. *J. Hosp. Infect.* **2009,** *71* (4), 295-300.
5. Cloutier, M.; Mantovani, D.; Rosei, F., Antibacterial Coatings: Challenges, Perspectives, and Opportunities. *Trends Biotechnol.* **2015,** *33* (11), 637-652.
6. Imani, S. M.; Ladouceur, L.; Marshall, T.; Maclachlan, R.; Soleymani, L.; Didar, T. F., Antimicrobial Nanomaterials and Coatings: Current Mechanisms and Future Perspectives to Control the Spread of Viruses Including SARS-CoV-2. *ACS Nano* **2020,** *14* (10), 12341-12369.
7. Huang, H.; Barber, O. W.; Yu, Z.; Park, H.; Hu, X.; Chen, X.; Chen, C.-H.; Hartmann, E. M.; Huang, J., Rub-Resistant Antibacterial Surface Conversion Layer on Stainless Steel. *Adv. Mater. Interfaces* **2022,** *9* (11), 2200251.
8. Mondschein, J. S.; Callejas, J. F.; Read, C. G.; Chen, J. Y. C.; Holder, C. F.; Badding, C. K.; Schaak, R. E., Crystalline Cobalt Oxide Films for Sustained Electrocatalytic Oxygen Evolution under Strongly Acidic Conditions. *Chem. Mater.* **2017,** *29* (3), 950-957.
9. Hassan, I. A.; Sathasivam, S.; Nair, S. P.; Carmalt, C. J., Antimicrobial Properties of Copper-Doped ZnO Coatings under Darkness and White Light Illumination. *ACS Omega* **2017,** *2* (8), 4556-4562.
10. Coll, M.; Napari, M., Atomic layer deposition of functional multicomponent oxides. *APL Mater.* **2019,** *7* (11), 110901.
11. Pickrahn, K. L.; Park, S. W.; Gorlin, Y.; Lee, H.-B.-R.; Jaramillo, T. F.; Bent, S. F., Active MnOx Electrocatalysts Prepared by Atomic Layer Deposition for Oxygen Evolution and Oxygen Reduction Reactions. *Adv. Energy Mater.* **2012,** *2* (10), 1269-1277.
12. Stevens, M. B.; Enman, L. J.; Batchellor, A. S.; Cosby, M. R.; Vise, A. E.; Trang, C. D. M.; Boettcher, S. W., Measurement Techniques for the Study of Thin Film Heterogeneous Water Oxidation Electrocatalysts. *Chem. Mater.* **2017,** *29* (1), 120-140.
13. Smith, R. D. L.; Prévot, M. S.; Fagan, R. D.; Zhang, Z.; Sedach, P. A.; Siu, M. K. J.; Trudel, S.; Berlinguette, C. P., Photochemical Route for Accessing Amorphous Metal Oxide Materials for Water Oxidation Catalysis. *Science* **2013,** *340* (6128), 60-63.

14. Jia, Q. X.; McCleskey, T. M.; Burrell, A. K.; Lin, Y.; Collis, G. E.; Wang, H.; Li, A. D. Q.; Foltyn, S. R., Polymer-assisted deposition of metal-oxide films. *Nat. Mater.* **2004,** *3* (8), 529-532.
15. Trotochaud, L.; Ranney, J. K.; Williams, K. N.; Boettcher, S. W., Solution-Cast Metal Oxide Thin Film Electrocatalysts for Oxygen Evolution. *J. Am. Chem. Soc.* **2012,** *134* (41), 17253-17261.
16. Lemire, J. A.; Harrison, J. J.; Turner, R. J., Antimicrobial activity of metals: mechanisms, molecular targets and applications. *Nat. Rev. Microbiol.* **2013,** *11* (6), 371-384.
17. Samani, S.; Hossainalipour, S. M.; Tamizifar, M.; Rezaie, H. R., In vitro antibacterial evaluation of sol–gel-derived Zn-, Ag-, and (Zn + Ag)-doped hydroxyapatite coatings against methicillin-resistant Staphylococcus aureus. *J. Biomed. Mater. Res., Part A* **2013,** *101A* (1), 222-230.
18. Dibrov, P.; Dzioba, J.; Gosink, K. K.; Häse, C. C., Chemiosmotic Mechanism of Antimicrobial Activity of Ag^{+} in Vibrio cholerae. *Antimicrob. Agents Chemother.* **2002**, *46* (8), 2668-2670.
19. Xiu, Z.-m.; Zhang, Q.-b.; Puppala, H. L.; Colvin, V. L.; Alvarez, P. J. J. Negligible Particle-Specific Antibacterial Activity of Silver Nanoparticles. *Nano Lett.* **2012**, *12*, 4271-4275.
20. Fang, L.; Cai, P.; Chen, W.; Liang, W.; Hong, Z.; Huang, Q. Impact of Cell Wall Structure on the Behavior of Bacterial Cells in the Binding of Copper and Cadmium. *Colloids Surf., A* **2009**, *347* (1), 50−55
21. Xi, J.; Wei, G.; An, L.; Xu, Z.; Xu Z.; Fan, L.; Gao, L. Copper/Carbon Hybrid Nanozyme: Tuning Catalytic Activity by the Copper State for Antibacterial Therapy. *Nano Lett.* **2019**, *19*, 7645−7654
22. Raghupathi, K. R.; Koodali, R. T.; Manna, A. C. Size-Dependent Bacterial Growth Inhibition and Mechanism of Antibacterial Activity of Zinc Oxide Nanoparticles. *Langmuir* **2011**, 27, 4020-4028
23. Sehmi, S. K.; Lourenco, C.; Alkhuder, K.; Pike, S. D.; Noimark, S.; Williams, C. K.; Shaffer, M. S. P.; Parkin, I. P.; MacRobert, A. J.; Allan, E. Antibacterial Surfaces with Activity against Antimicrobial Resistant Bacterial Pathogens and Endospores. *ACS Infet. Dis.* **2020**, *6*, 939-946.
24. Ghosh, R.; Swart, O.; Westgate, S.; Miller, B. L.; Yates, M. Z., Antibacterial Copper–Hydroxyapatite Composite Coatings via Electrochemical Synthesis. *Langmuir* **2019,** *35* (17), 5957-5966.
25. Geuli, O.; Lewinstein, I.; Mandler, D., Composition-Tailoring of ZnO-Hydroxyapatite Nanocomposite as Bioactive and Antibacterial Coating. *ACS Appl. Nano Mater.* **2019,** *2* (5), 2946-2957.
26. McGee, S.; Lei, Y.; Goff, J.; Wilkinson, C. J.; Nova, N. N.; Kindle, C. M.; Zhang, F.; Fujisawa, K.; Dimitrov, E.; Sinnott, S. B.; Dabo, I.; Terrones, M.; Zarzar, L. D., Single-Step Direct Laser Writing of Multimetal Oxygen Evolution Catalysts from Liquid Precursors. *ACS Nano* **2021,** *15* (6), 9796-9807.
27. Kast, M. G.; Cochran, E. A.; Enman, L. J.; Mitchson, G.; Ditto, J.; Siefe, C.; Plassmeyer, P. N.; Greenaway, A. L.; Johnson, D. C.; Page, C. J.; Boettcher, S. W., Amorphous Mixed-Metal Oxide Thin Films from Aqueous Solution Precursors with Near-Atomic Smoothness. *J. Am. Chem. Soc.* **2016,** *138* (51), 16800-16808.

28. Jhang, R.-H.; Yang, C.-Y.; Shih, M.-C.; Ho, J.-Q.; Tsai, Y.-T.; Chen, C.-H., Redox-assisted multicomponent deposition of ultrathin amorphous metal oxides on arbitrary substrates: highly durable cobalt manganese oxyhydroxide for efficient oxygen evolution. *J. Mater. Chem. A* **2018,** *6* (37), 17915-17928.
29. Shih, M.-C.; Jhang, R.-H.; Tsai, Y.-T.; Huang, C.-W.; Hung, Y.-J.; Liao, M.-Y.; Huang, J.; Chen, C.-H., Discontinuity-Enhanced Thin Film Electrocatalytic Oxygen Evolution. *Small* **2019,** *15* (50), 1903363.
30. Zegeye, T. A.; Chen, W.-T.; Hsu, C.-C.; Valinton, J. A. A.; Chen, C.-H., Activation Energy Assessing Potential-Dependent Activities and Site Reconstruction for Oxygen Evolution. *ACS Energy Lett.* **2022**, 2236-2243.
31. Suib, S. L., Porous Manganese Oxide Octahedral Molecular Sieves and Octahedral Layered Materials. *Acc. Chem. Res.* **2008,** *41* (4), 479-487.
32. Yeh, C.-H.; Hsu, W.-Y.; Hsu, C.-C.; Valinton, J. A. A.; Yang, C.-I.; Chiu, C.-c.; Chen, C.-H., Cobalt Iron Oxides Prepared by Acidic Redox-Assisted Precipitation: Characterization, Applications, and New Opportunities. *ACS Appl. Mater. Interfaces* **2021,** *13* (44), 52181-52192.
33. Hwang, B.-U.; Zabeeb, A.; Trung, T. Q.; Wen, L.; Lee, J. D.; Choi, Y.-I.; Lee, H.-B.; Kim, J. H.; Han, J. G.; Lee, N.-E., A transparent stretchable sensor for distinguishable detection of touch and pressure by capacitive and piezoresistive signal transduction. *NPG Asia Mater.* **2019,** *11* (1), 23.
34. Mobile Touches - dscout's inaugural study on humans and their tech. https://dscout.com/people-nerds/mobile-touches (accessed 2022-06-13).
35. Cleaning and disinfection of environmental surfaces in the context of COVID-19. https://www.who.int/publications/i/item/cleaning-and-disinfection-of-environmental-surfaces-inthe-context-of-covid-19.
36. Skoog, D. A.; West, D. M.; Holler, F. J.; Crouch, S. R. Applications of Oxidation/Reduction Titrations. In *Fundamentals of Analytical Chemistry*, 9th ed.; Brooks/Cole, 2014; pp. 509-534.
37. Warnes, S. L.; Little, Z. R.; Keevil, C. W.; Colwell, R., Human Coronavirus 229E Remains Infectious on Common Touch Surface Materials. *mBio* **2015,** *6* (6), e01697-15.
38. Govind, V.; Bharadwaj, S.; Sai Ganesh, M. R.; Vishnu, J.; Shankar, K. V.; Shankar, B.; Rajesh, R., Antiviral properties of copper and its alloys to inactivate covid-19 virus: a review. *Biometals* **2021,** *34* (6), 1217-1235.
39. Hochmannova, L.; Vytrasova, J., Photocatalytic and antimicrobial effects of interior paints. *Prog. Org. Coat.* **2010,** *67* (1), 1-5.
40. Chata, G.; Nichols, F.; Mercado, R.; Assafa, T.; Millhauser, G. L.; Saltikov, C.; Chen, S., Photodynamic Activity of Graphene Oxide/Polyaniline/Manganese Oxide Ternary Composites toward Both Gram-Positive and Gram-Negative Bacteria. *ACS Appl. Bio Mater.* **2021,** *4* (9), 7025-7033.
41. Singh, J.; Hegde, P. B.; Ravindra, P.; Sen, P.; Avasthi, S., Ambient Light-Activated Antibacterial Material: Manganese Vanadium Oxide ($Mn_2V_2O_7$). *ACS Appl. Bio Mater.* **2021,** *4* (9), 6903-6911.
42. Ning, C.; Wang, X.; Li, L.; Zhu, Y.; Li, M.; Yu, P.; Zhou, L.; Zhou, Z.; Chen, J.; Tan, G.; Zhang, Y.; Wang, Y.; Mao, C. Concentration Ranges of Antibacterial Cations for Showing the Highest Antibacterial Efficacy but the Least Cytotoxicity against

Mammalian Cells: Implications for a New Antibacterial Mechanism. *Chem. Res. Toxicol.* **2015**, *28*, 1815-1822.
43. Agarwal, A.; Weis, T. L.; Schurr, M. J.; Faith, N. G.; Czuprynski, C. J.; McAnulty, J. F.; Murphy, C. J.; Abbott, N. L. Surfaces modified with nanometer-thick silver-impregnated polymeric films that kill bacteria but support growth of mammalian cells. *Biomaterials* **2010**, *31*, 680−690.
44. Song, W.; Zhang, J.; Guo, J.; Zhang, J.; Ding, F.; Li, L.; Sun, Z. Role of the dissolved zinc ion and reactive oxygen species in cytotoxicity of ZnO nanoparticles. *Toxicol. Lett.* **2010**, *199*, 389−397.
45. Burghardt, I.; Lüthen, F.; Prinz, C.; Kreikemeyer, B.; Zietz, C.; Neumann, H.-G.; Rychly, J. A dual function of copper in designing regenerative implants. *Biomaterials* **2015**, *44*, 36−44.
46. Friedlander, R. S.; Vogel, N.; Aizenberg, J., Role of Flagella in Adhesion of Escherichia coli to Abiotic Surfaces. *Langmuir* **2015,** *31* (22), 6137-6144.
47. Toyofuku, M.; Nomura, N.; Eberl, L., Types and origins of bacterial membrane vesicles. *Nat. Rev. Microbiol.* **2019,** *17* (1), 13-24.

TABLE OF CONTENTS GRAPHIC